Horseshoe chaos in a bistable optical system under a modulated incident field

Majid Taki*
Laboratoire de Spectroscopie Hertzienne, CNRS URA 249, Université des Sciences et Technologies de Lille, UFR de Physique, Bâtiment P5, F-59655 Villeneuve d'Ascq Cédex, France
(Received 10 December 1996; revised manuscript received 23 June 1997)

It is shown analytically and numerically that a single-mode bistable optical system, under a modulated incident field, may undergo a chaotical behavior of Smale horseshoe type. The threshold for the onset of chaos and the bifurcating curves for nonlinear resonances are derived semianalytically, by means of the Melnikov method, and numerically checked. We also demonstrate the existence of multistable attractors. Two time-periodic states and a strange attractor are shown to coexist for a certain range of parameters. [S1063-651X(97)08310-4]

PACS number(s): 42.65.Sf

I. INTRODUCTION

The response of nonlinear dynamical systems to external periodic forcing may exhibit a large variety of complex behavior, including phase-locked phenomena, quasiperiodicity, and chaos. In particular, dynamic chaos has been detected in a large number of nonlinear systems of various natures. One of these problems that has been studied extensively is optical bistability (OB) [1–4]. In fact, optical bistability has become one of the most active fields in nonlinear optics not only for the richness in nonlinear dynamical behaviors [5–7] but also for the potential applications of bistable optical devices [8,9]. Indeed, even slow and moderate modulations of the incident field may have a great benefit for signal amplifications in such optical systems. The recent and growing progress in nonlinear optics and particularly in laser systems renders them serious and promising candidates for making operating devices smaller and faster [10]. However, it is well known that bistable optical systems can exhibit, in addition to regular states, complex chaotic attractors. Even though, in general, these complex systems have high-dimensional phase space, their chaotic attractors are often low dimensional and reduced dynamical models still provide a good theoretical description of experimental observations [11,12]. In this paper we are interested in the effects of time-periodic modulations of the applied incident field on the chaotical dynamic of a passive optical bistable system. More specifically, we consider a bistable optical system consisting of an optical unidirectional ring cavity filled with a passive medium, consisting of a collection of homogeneously broadened two-level atoms and subjected to an incident field whose amplitude is time modulated. We focus on the study of the interaction between periodic modulations of the incident field and the homoclinic orbit leading to properties involving the global aspects of the dynamic and show that the situation may become drastic, even for a reduced dynamical model. We show that the main features are the phase-locked phenomena leading to nonlinear resonance dynamics and transitions from a regular to a chaotic regime. We show also that the chaotic regime is of Smale horseshoe type and derive semianalytical expressions for the threshold of the onset of chaos by means of Melnikov's method. If the amplitude of the modulation is large enough to overcome the dissipation (absorptive terms and losses in the cavity) then the system may exhibit multistable attractors consisting of two time-periodic states and a strange attractor. As a result, one may expect first that switching phenomena may occur between complex attractors (appearing when modulations are present). Second, the transverse intersections between stable and unstable manifolds (separatrices) may give rise to chaotic transport throughout some particular regions of phase space. More precisely, in the absence of modulations, the homoclinic orbit separates the phase-space portrait in three regions. The motions are qualitatively different in each one. Furthermore, any initial condition starting in one region remains in it forever. On the contrary, under time-periodic amplitude modulations, the underlying homoclinic orbit ''breaks up,'' leading to transverse intersections between its stable and unstable manifolds, and in particular chaotic regimes make it possible for motions inside the homoclinic orbit to escape it. Similarly, motions outside the homoclinic orbit may enter it. This gives rise to the phenomenon of transport in phase space between regions exhibiting qualitatively different motions (for more details about transport theory see Ref. [13]). One consequence for bistable optical systems is that the input power for commutation may be considerably lower under small time-periodic amplitude modulations.

The rest of the paper is organized as follows. In Sec. II we give a physical description of the problem. Section III provides a brief review of Melnikov's techniques. Section IV contains the analytical treatments for both the homoclinic orbit and the resulting horseshoe chaos in the system. The same approach is applied to study the nonlinear resonances and the coexistence between time-periodic states and a strange attractor. Numerical results and a comparison with analytical predictions are given. Concluding remarks constitute Sec. V.

II. PHYSICAL DESCRIPTION OF THE PROBLEM

A. Physical model

In this study we consider an OB system that contains an optical unidirectional cavity filled with a passive medium,

*Electronic address: taki@lsh.univ-lille1.fr

consisting of homogeneously broadened two-level atoms and driven by an external optical signal whose amplitude is time-periodic modulated. Assuming that the resonant cavity is operating in a single mode and using the plane-wave approximation together with the mean-field limit, we can reduce the Maxwell-Bloch equations [14] to

$$\frac{dF}{dt}=\kappa[y-(1+i\theta)F-2CP], \tag{1a}$$

$$\frac{dP}{dt}=\gamma_{\perp}[FD-(1+i\Delta)P], \tag{1b}$$

$$\frac{dD}{dt}=-\gamma_{\parallel}\left[\frac{1}{2}(FP^{*}+F^{*}P)+D-1\right], \tag{1c}$$

where F, D, and P are the normalized slowly varying envelopes of the electric field, of the population difference, and of the molecular polarization, respectively. The parameter C is the bistability parameter, κ is the cavity linewidth, and $\gamma_{\parallel}$ and $\gamma_{\perp}$ are the relaxation rates of the population difference and polarization. The frequencies of the external field, the cavity, and the atoms are denoted by ω_0, ω_c, and ω_a, respectively. The two detuning parameters are defined as $\Delta=(\omega_a-\omega_0)/\gamma_{\perp}$ and $\theta=(\omega_c-\omega_0)/\gamma_{\perp}$. The normalized amplitude of the external field y is assumed to be real and time-periodic modulated. In the absence of modulations, Eq. (1) was derived by Bonifacio, Granchi, and Lugiato [15] as a one-mode theory of optical bistability and has been extensively studied in a number of applications. In fact, they predict absorptive as well as dispersive bistability and the results are qualitatively and quantitatively in rather good agreement with the experimental observations [11,12]. It has been shown that since the bistability parameter is large enough, in the absence of modulations, Eq. (1) undergoes a period-doubling route to chaos. Many authors have studied the chaotic dynamics of Eq. (1) for different ranges of control parameters. Gang, Ning, and Haken [16] have analyzed the instability regions in detail and revealed that chaotic attractors may coexsist with time-periodic orbits leading to bistability and even tristability phenomena. In the present work, however, we are interested in the effects of time-periodic modulations on the input field, which greatly complicate the situation. First, it is well known that external modulations favor the nonlinear resonances leading to the selection between time-periodic attractors. Second, optical systems with modulated parameters often exhibit experimental chaotic motion for a large range of parameters including both active (lasers) [17] and passive optical systems. Moreover, chaotic motions have already been experimentally observed in a passive optical bistable system under a frequency-modulated input field [18]. The authors have shown numerically that Eq. (1) reproduces fairly well their experimental observations including chaotic regimes. Still, a number of important questions remain to be answered. What is the nature of choas appearing in the system? Is it possible to predict the threshold of the onset of chaos? What is the structure of the attracting basins? In order to attempt to answer these questions we concentrate on the reduced model of the good cavity limit, which constitutes a simplified version of Eq. (1), and assume that the amplitude of the input field is time-periodic modulated. Still, this model captures the main features of the nonlinear dynamics appearing in the system.

B. Reduced model system

In order to keep the analysis as simple as possible, we consider the good cavity case where $\kappa \ll \gamma_{\parallel}, \gamma_{\perp}$. In this situation the atomic variables vary in time much more rapidly than the field variables and can be eliminated by setting $dP/dt=dD/dt=0$ in Eq. (1). Thus one obtains the relations

$$P_s=\frac{(1-i\Delta)F}{1+\Delta^2+|F|^2}, \quad D_2=\frac{1+\Delta^2}{1+\Delta^2+|F|^2}$$

and the self-contained equation for the field

$$\kappa^{-1}\frac{dF}{dt}=y-F\left[1+\frac{2C}{1+\Delta^2+|F|^2}+i\left(\theta-\frac{2C\Delta}{1+\Delta^2+|F|^2}\right)\right]. \tag{2}$$

For the sake of simplicity, let us consider conditions of purely dispersive OB [15]:

$$\Delta^2 \gg 1, \quad \Delta\theta \gg 1, \quad \theta \ll \Delta. \tag{3}$$

In this case, in order to go further into the analysis, it is convenient to write Eq. (2) in a simplified form. Hence we rescale F, y, and t by setting $\tau=\kappa\theta t$, $X=(\theta/2C\Delta)^{1/2}F$, and $Y=(\theta/2C\Delta)^{1/2}(y/\theta)$. We write Eq. (2) as a first-order system

$$\frac{dx_1}{d\tau}=Y_0+x_2\left(1-\frac{1}{a+|X|^2}\right)-\varepsilon\left[x_1\left(\delta_1+\frac{\delta_2}{a+|X|^2}\right)+A\sin\omega\tau\right], \tag{4a}$$

$$\frac{dx_2}{d\tau}=-x_1\left(1-\frac{1}{a+|X|^2}\right)-\varepsilon x_2\left(\delta_1+\frac{\delta_2}{a+|X|^2}\right), \tag{4b}$$

where $a=(1+\Delta^2)\theta/2C\Delta$, $\delta_1\varepsilon=1/\theta$, and $\delta_2\varepsilon=1/\Delta$. The amplitude modulation is written in the form $Y=Y_0+\varepsilon A\sin\omega\tau$, where ε is a small parameter, εA is the modulation of the scaled field Y, and the scaled field variable $X=x_1+ix_2$. Note that the third relation in the conditions (3) of purely dispersive OB leads to $\delta_1 \gg \delta_2$, which means that the two terms in Eq. (4) where δ_2 appears may be neglected. In order to extend our analytical analysis to the case where all terms are significant, we will take Δ and θ large enough but of the same order of magnitude. Melnikov's method is independent of the relative order of magnitude in perturbative terms. In addition, we are not interested in the unperturbed ($\varepsilon=0$) system in itself; it serves mainly to approximate the analytical form of the homoclinic orbits. In fact, when $\varepsilon=0$, the unperturbed system (Fig. 1) has already been used by Lugiato, Milani, and Meystre [19] as a basic system to derive the analytical threshold for anomalous switching in dispersive optical bistability. Furthermore, the unperturbed problem cannot describe optical bistability because of the marginal instability of the stationary solutions due to the lack of dissipation. However, it contains the homoclinic orbit, which is responsible for the anomalous switching phenom-

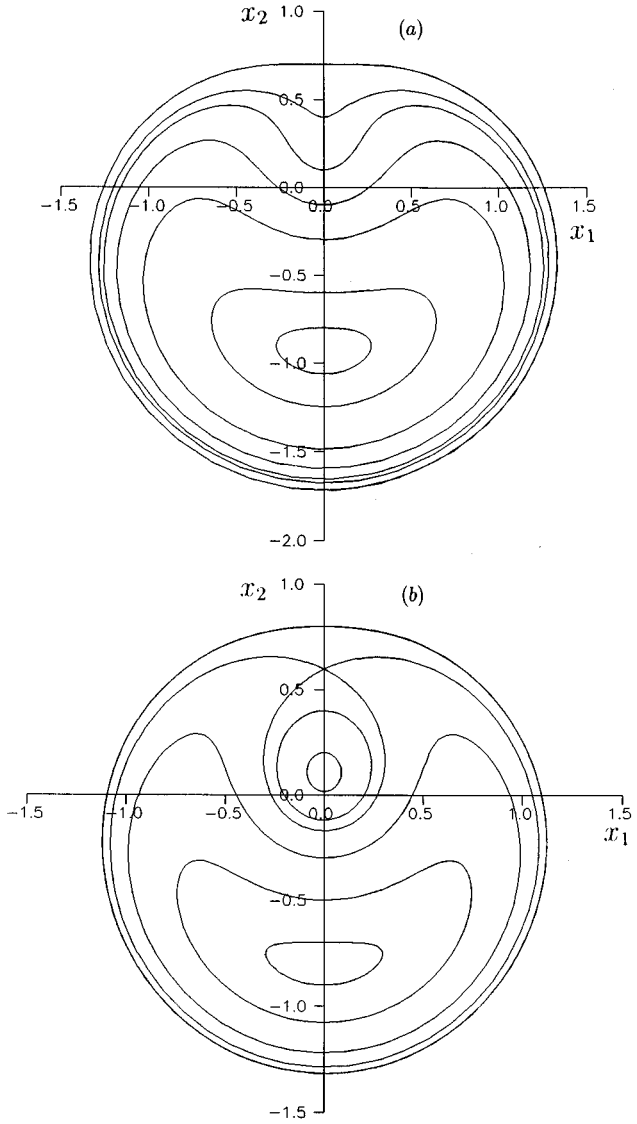

FIG. 1. Phase space of the unperturbed ($\varepsilon=0$) system (4). A family of level curves is shown, when $a=0.5$. One stationary solution is for (a) $Y_0=0.25>Y_c$, while the double homoclinic connection is shown for (b) $Y_0=0.1<Y_c$.

enon, as pointed out in Ref. [19]. Here we show that homoclinic orbits still play a crucial role in the chaotic behavior of the perturbed system when the competition between dissipation (absorptive terms and losses in the cavity) and modulation has been restored. Indeed, the homoclinic orbits are related to global aspects of the dynamic. So, in the following analysis of the chaotic regimes and nonlinear resonances leading to it, we will use global perturbation techniques originally due to Melnikov [20].

III. MELNIKOV'S METHOD: PERTURBATIONS OF PLANAR HOMOCLINIC AND PERIODIC ORBITS

Melnikov's method is now widely described in classical books and papers [21,22]. In this section we briefly review the analytical techniques to be used below. For some typical applications in physics and fluid mechanics see Ref. [23]; see also Ref. [24] for very recent developments of Melnikov's techniques.

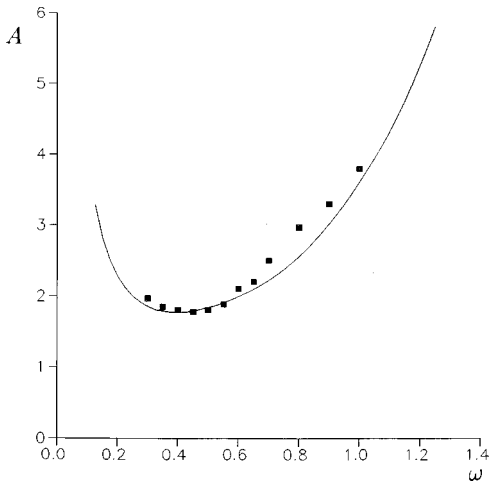

FIG. 2. Critical curve for the onset of chaos, in the parameter plane (A,ω) of the external field input. Discrete symbols correspond to numerical thresholds of chaos. The critical curve for the outer homoclinic loop is not shown in the figure. It is just a translated curve, toward high values of A, of that of the inner one. For comparison and clarity we have set the other parameters to $a=0.5$, $\delta_1=\delta_2=1$, $\varepsilon=0.05$, and $Y_0=0.1$ for all figures.

We consider a system of ordinary differential equations of the form

$$\frac{dX}{d\tau}=f(X)+\varepsilon g(X,\tau), \tag{5}$$

where $X=(u,v)$, $f=\binom{f_1(X)}{f_2(X)}$, $g=\binom{g_1(X,\tau)}{g_2(X,\tau)}$, and g is periodic in time of period T. Assume that, for $\varepsilon=0$, the above system possesses a homoclinic orbit (separatrix) $X_h(\tau)$ to hyperbolic saddle point p_0 (or homoclinic cycles) and a continuous family of periodic orbits $X_\alpha(\tau)$ in the interior of $X_h(\tau)$. Therefore, Melnikov's function is defined as

$$M(\tau_0)=\int_{-\infty}^{+\infty} f(X_h(\tau))\wedge g(X_h(\tau),\tau+\tau_0)d\tau, \tag{6}$$

where the wedge product is defined as $X_1\wedge X_2=u_1v_2-u_2v_1$. Note that the initial time τ_0 appears explicitly since solutions of Eq. (5) are not invariant under time translations. Furthermore, τ_0 is used for the parametrization of the Poincaré section, which is constructed by sampling the coordinates u,v each time the function g completes one period. In fact, $M(\tau_0)$ provides a good mesure [to $O(\varepsilon^2)$], in the Poincaré section, of the distance $d(\tau_0)$ between the stable and unstable perturbed manifolds, which is defined as

$$d(\tau_0)=\varepsilon\,\frac{M(\tau_0)}{|f(X_0(0))|}+O(\varepsilon^2). \tag{7}$$

In the same spirit the existence of the periodic orbits $X_\alpha(\tau)$ of period mT/n (the subharmonics) is evaluated by the subharmonic Melnikov function

$$M^{m/n}(\tau_0)=\int_0^{mT} f(X_\alpha(\tau))\wedge(X_\alpha(\tau),\tau+\tau_0)d\tau. \tag{8}$$

Therefore, simple zeros of $M(\tau_0)$ correspond to transverse intersections of stable and unstable manifolds leading to Smale horseshoe chaos [21], while those of $M^{m/n}(\tau_0)$ give rise to subharmonic orbits of period mT.

IV. TEMPORAL CHAOS AND NONLINEAR RESONANCES

A. Smale horseshoe chaos

We return now to system (4). When $\varepsilon=0$, the unperturbed Hamiltonian reads

$$H(x_1,x_2)=\tfrac{1}{2}(x_1^2+x_2^2)+x_2Y_0-\tfrac{1}{2}\ \ln(a+x_1^2+x_2^2)+\text{const} \tag{9}$$

and constitutes a one-parameter family of level curves in phase space (x_1,x_2). The examination of the stationary fixed points leads to the bistability conditions, namely, $a<1$ and $Y_0<Y_c$, where

$$Y_c^2=(-a-\tfrac{1}{2}+\sqrt{2a+\tfrac{1}{4}})\left(1-\frac{1}{-1+\sqrt{8a+1}}\right)^2. \tag{10}$$

When $a\geqslant 1$ no bistability can occur and we are not interested in this case. Figure 1 displays the phase space showing two different situations with typical values of the parameters a and Y_0. Note the double homoclinic connection, via a saddle point, of the two homoclinic loops. This situation is highly degenerate since each homoclinic loop is formed by the coincidence of the stable and unstable manifolds of the saddle fixed point. Hence one would expect them to break up under the influence of input field amplitude modulations and dissipative terms. According to Sec. III, we use Melnikov's method to evaluate the threshold of chaos arising from transverse intersections of the stable and unstable manifolds [21]. We now intruduce the Melnikov function $M(\tau_0)$ for the homoclinic loops $X_h=(x_{1,h},x_{2,h})$ (setting h for both inner and outer loops):

$$\begin{aligned}M(\tau_0)=&-\int_{-\infty}^{+\infty}\left(\delta_1+\frac{\delta_2}{a+|X_h|^2}\right)\left[y_0x_{2,h}\right.\\&\left.+\left(1-\frac{1}{a+|X_h|^2}\right)\left|X_h\right|^2\right]d\tau\\&+A\ \cos\omega\tau_0\int_{-\infty}^{+\infty}\left(1-\frac{1}{a+|X_h|^2}\right)x_{1,h}\ \sin\omega\tau\ d\tau\\=&I_1+I_2A\ \cos\ \omega\tau_0,\end{aligned}$$

where I_1 and I_2 are the first and second integrals, respectively. Therefore, simple zeros of $M(\tau_0)$ are characterized by the relation $A>|I_1/I_2|=A_c$, where A_c can be viewed as being the minimum amplitude modulation (minimum modulated input power) necessary for the system to transit from regular to chaotic regimes. To evaluate the integrals I_1 and I_2, one needs the analytical forms of the homoclinic loops X_h, which are determined by Eq. (9). Unfortunately, their time dependence cannot be obtained in an explicit form. Therefore, we will calculate them numerically, using an approach similar to that used by Taki, Fernandez, and Reinisch in [23]. We emphasize that we have systematically checked

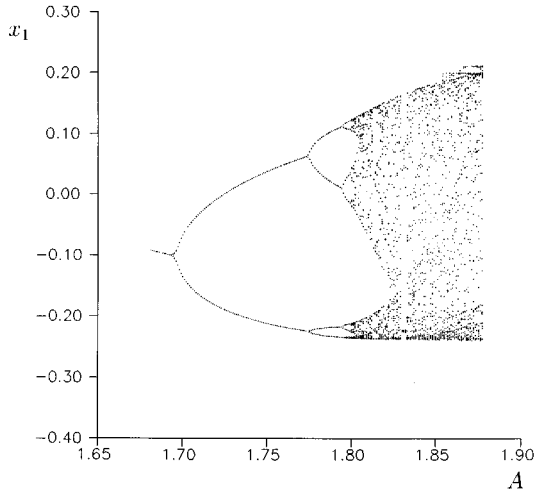

FIG. 3. Bifurcation diagram in the Poincaré section of the real part x_1 of the electric field versus the amplitude A of the modulation with $\omega=0.5$. The Poincaré section is constructed by sampling the coordinate x_1 each time the input field completes one period.

the analytical predictions for different values of the small parameter ε and we have observed that the accuracy decreased by increasing ε. This is obvious from the fact that Melnikov's method is a first-order method for the small parameter ε [see Eq. (7) in Sec. III]. Also, in the following numerical simulations we have set the parameters to typical values $a=0.5$, $Y_0=0.1$, $\delta_1=\delta_2=1$, and $\varepsilon=0.05$. The input field parameters A and ω are control parameters. Figure 2 shows the critical curve for the onset of chaos, which separates the parameter plane (A,ω) into two regions, namely, the upper region where the stable and unstable perturbed manifolds intersect transversely, since $M(\tau_0)$ has simple zeros, and the system (4), which exhibits chaotic behaviors. There exist, in the phase space, sets of chaotic orbits that are of Smale horseshoe type [21]. In the lower region no intersection can occur at all. Transitions between these two regions occur by a homoclinic bifurcation. More precisely, the last case gives the main result of Melnikov's theory that, for any parameter in that region, the whole system is not chaotic. Thus, for all initial conditions the behavior is regular and globally related to planar systems whose typical behaviors are fairly well understood. In particular, we recover the classical S-shaped bistability curve. Note that it is easy to verify, by using the Poincaré-Bendixon criterion, that there are no periodic or homoclinic orbits and the only attractors are the fixed points in the Poincaré sections, namely, the resonant and the forced steady-state oscillations that originate from the stable equilibrium states. We have not shown the critical curve for the outer homoclinic loop, which is similar to that of the inner one translated toward high values of the amplitude A. Chaos has been investigated numerically for different sets of parameters, and numerical thresholds for typical frequencies are also illustrated in Fig. 2, which are in very good agreement with the critical curve for the onset of chaos. Although the agreement is satisfactory, we have observed that Melnikov's technique provides a good, but slightly low, estimate of the chaos threshold. Hence we have integrated the system (4) for different sets of parameter values and this tendency is confirmed. This might be understood by the fact that at the onset of chaos the attracting basin of the chaotic

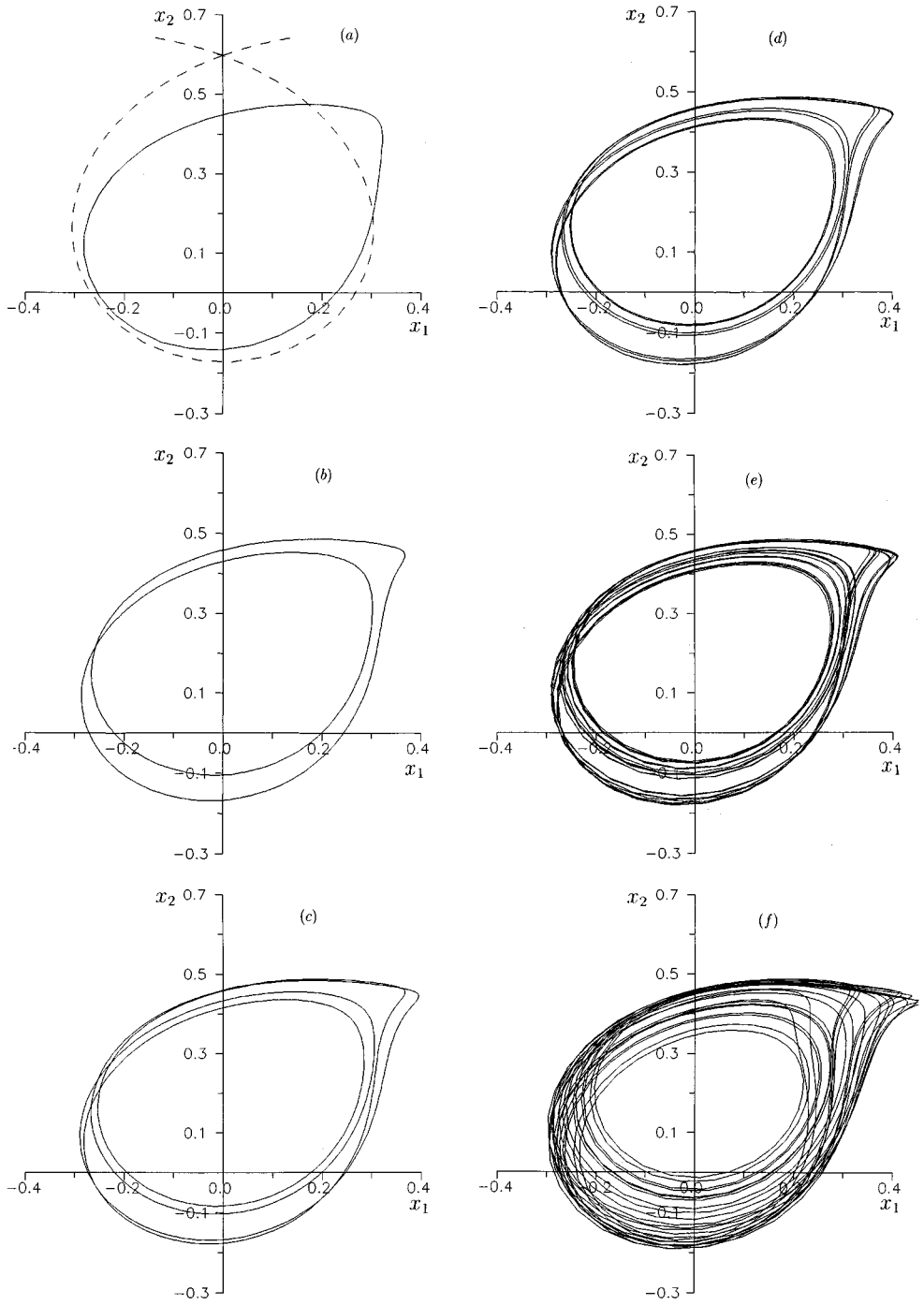

FIG. 4. Sequence of period doubling in the Poincaré section defined in Fig. 3. The unperturbed (i.e., $\varepsilon = 0$) inner homoclinic loop is dashed in (a) for reference. A is increased from (a) 1.7, (b) 1.75, (c) 1.79, (d) 1.797, (e) 1.81, and (f) 1.88, corresponding to the $1T$, $2T$, $4T$, and $8T$ transitions, chaos, and chaos, respectively.

regime constitutes a small set of phase space that renders the numerical observation of chaos at the threshold very difficult. We also have numerically integrated the system (4) in order to characterize the nature of transitions from regular to chaotic regimes by increasing from zero the amplitude A of the field amplitude modulation. The only route to chaos we have observed is the classical period-doubling route as displayed in Figs. 3 and 4 for a typical value of the frequency of the modulation. However, when A is further increased the chaotic behavior develops (see Fig. 3) and a different stable periodic state appears. Concerning this different periodic state, we have observed, at the coexistence threshold, a long-time chaotic transient that disappears under a small increment of the amplitude A, as shown in Fig. 5. This important feature of the coexistence of time-periodic states and a strange attractor for a certain range of parameters that is related to nonlinear resonances will be discussed in the next subsection.

B. Nonlinear resonances

We have observed in the preceding subsection that the Smale horseshoe chaos may be related to a sequence of sub-

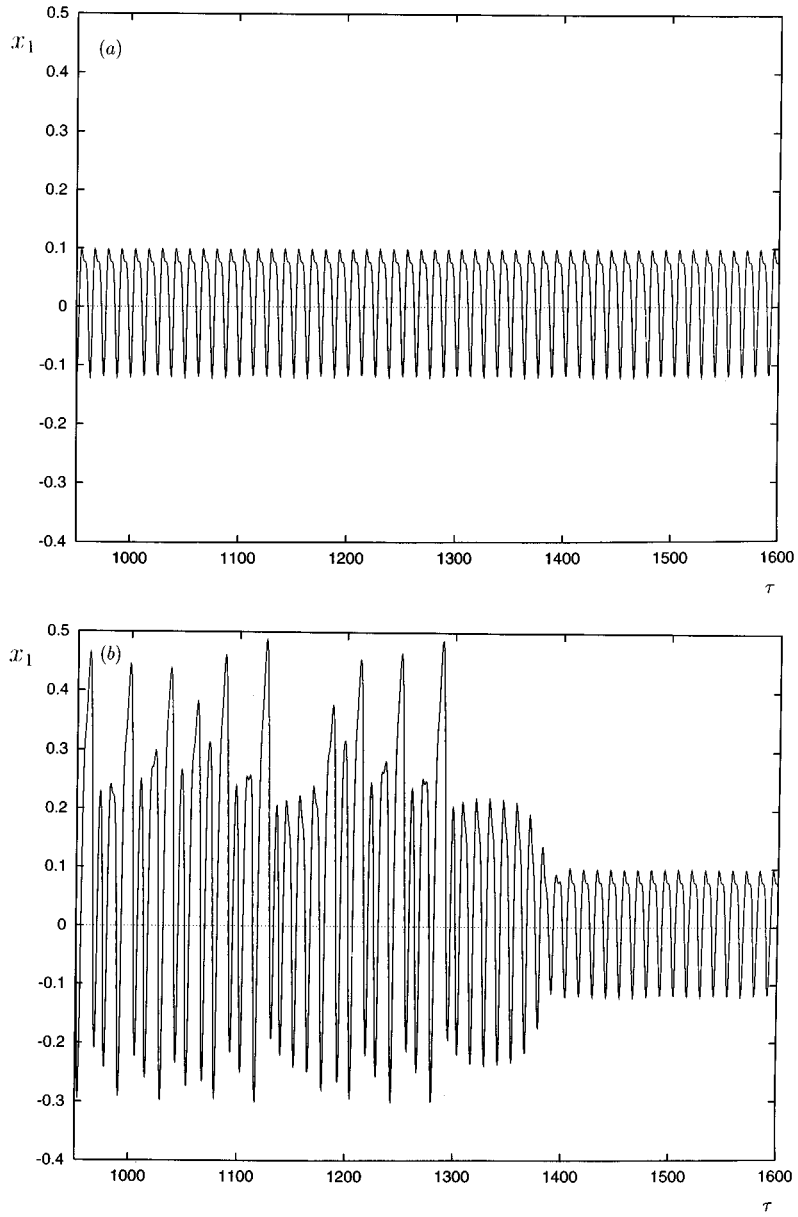

FIG. 5. Chaotic transients of the real part x_1 of the electric field under a small increment of the amplitude of the modulation. (a) The asymptotic state restabilizes on a $1T$ periodic state for $A=1.8802$. (b) Long-time transients chaos before stabilization on the $1T$ periodic state for $A=1.8801$. Both traces are made with the same initial condition and the parameters are the same as those of Fig. 4.

harmonic bifurcations, which are important for transitions both from linear to nonlinear resonances and from regular to chaotic behaviors. Thus, in this section we focus on the dynamics of large-amplitude periodic orbits inside the homoclinic loops. Again we have evaluated the subharmonic Melnikov function $M^{m/n}(\tau_0)$ defined by Eq. (8) in the preceding subsection, which enables us to detect the existence of subharmonics and the occurrence of their saddle-node bifurcations exactly. Hence simple zeros of $M^{m/n}(\tau_0)$ give rise to subharmonic solutions whose periods T_s are related to the period T of the modulation by the relation $T_s=(m/n)T$, where m and n are prime integers. In fact, the above simple zeros, in the parameter plane (A,ω), permit us to estimate the minimum values of the amplitude A of the modulation necessary for the occurrence of subharmonics. Figure 6 shows a comparison between Melnikov's predictions and the corresponding numerical simulations for the critical values of the amplitude A necessary for subharmonic orbits ($m=1$ and $n=1$) to exist, versus frequency. The agreement between predictions and numerical thresholds is satisfactory, except for low frequencies, where Melnikov's method provides slightly lower estimates. By increasing A from its critical value (for fixed ω), the resonant orbits undergo a repeated sequence of period doubling. When A is further increased the situation becomes more and more complicated. We have observed a coexistence between (i) different periodic states and (ii) periodic states and a chaotic attractor. This coexistence may be understood by the comparison between the critical curves for the existence of subharmonics on the one hand and the onset of chaos on the other. Indeed, the critical curve for the onset of chaos together with the critical curves for the occurrence of subharmonics, for three periodic orbits ($\omega_s=0.4$, 0.5 and 0.6) in the parameter plane (A,ω), are plotted in Fig. 7. Each curve separates the parameter plane into two

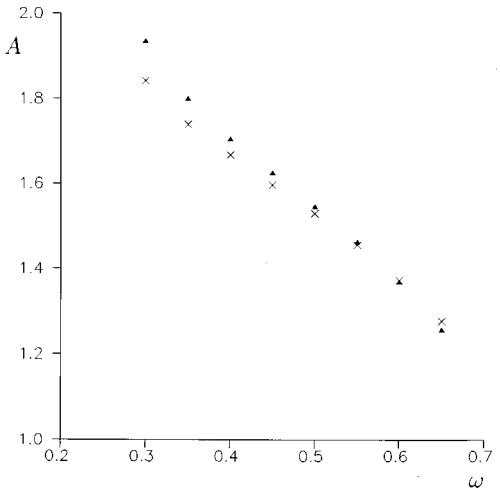

FIG. 6. Comparison between Melnikov's predictions (×) for the existence of subharmonic orbits ($m=n=1$) and the corresponding numerical thresholds (▲) in the parameter plane (A,ω). The values of the other parameters are given in Fig. 2.

regions. Chaotic regimes may occur in the upper region above the solid curve, while periodic states may exist in the upper region above each one of the other three curves. Of a great importance is the region where Melnikov's method predicts the existence of both subharmonics and chaos. In particular, in that region the system may exhibit a coexistence between a time-periodic state and a chaotic attractor, as shown in Fig. 8, where the results from both Figs. 2 and 6 are displayed in the same frame for comparison. Moreover, Fig. 9 illustrates a typical situation where two different time-periodic states coexist with a strange attractor for the same set of parameters. To get more insight into the coexistence of these states we have integrated the system (4) for different initial conditions and the complexity of the attracting basins is shown in Fig. 10. In addition, we have also observed multistability states characterized by the coexistence of two or three time-periodic states and a chaotic state. We emphasize that similar features, namely, homoclinic chaos, have been

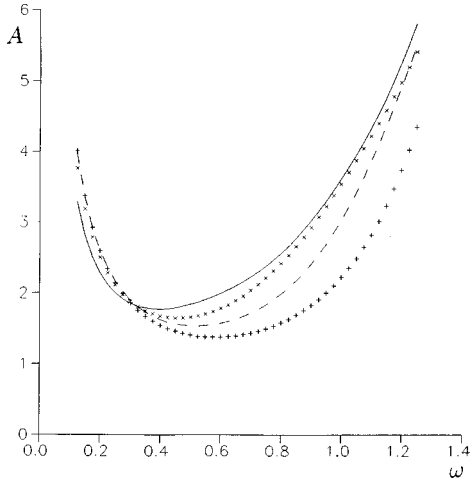

FIG. 7. Bifurcation curves for the inner homoclinic loop and subharmonics in the parameter plane (A,ω) for three typical time-periodic orbits of system (4): $\omega_s=0.6$ (+), $\omega_s=0.5$ (--), $\omega_s=0.4$ (×), and the homoclinic loop (—).

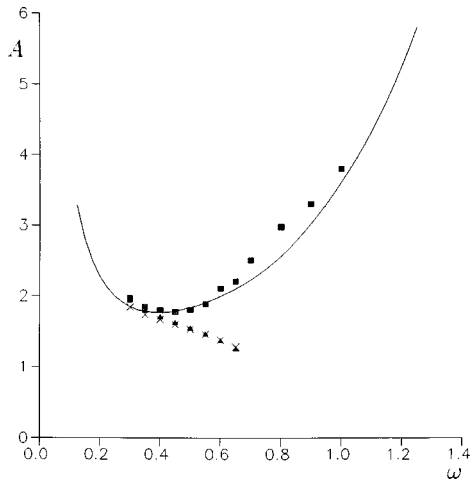

FIG. 8. Comparison between thresholds for chaos and the subharmonic existence, respectively. Shown are Melnikov's prediction of chaos (—), the corresponding numerical thresholds (■), Melnikov's thresholds for the subharmonics to exist (×), and the corresponding numerical thresholds (▲). Note the coexistence of time-periodic states and chaos.

observed experimentally in a bistable optical system whose input field is frequency modulated [26,18]. However, we have not observed abrupt transitions from $1T$-periodic state to chaos, which have also been observed experimentally [18], even though the analytical study does not exclude this situation. In fact, this transition has already been observed numerically for nonlinear Duffing oscillators [25], which may constitue an approximation of the system (4) under appropriate conditions [15].

V. CONCLUDING REMARKS

We have shown that, under time-periodic amplitude modulations of the input field, optical bistable systems in the good cavity limit may undergo a possible period-doubling route to chaos. We derived, by means of Melnikov's method, critical curves to the onset of chaos and nonlinear resonances leading to it by repeated subharmonic bifurcations. The chaos is of the homoclinic type, initiated by transverse inter-

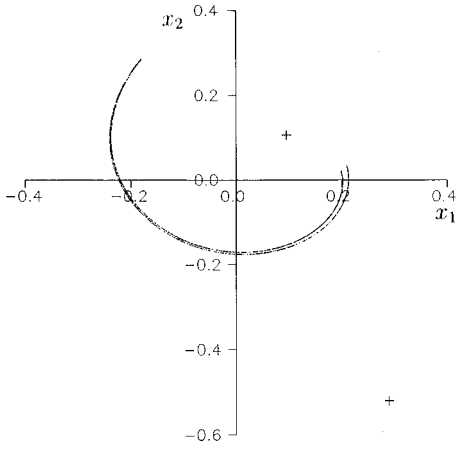

FIG. 9. Coexistence of a strange attractor and two time-periodic states in the Poincaré section defined in Fig. 3 with $A=1.877$.

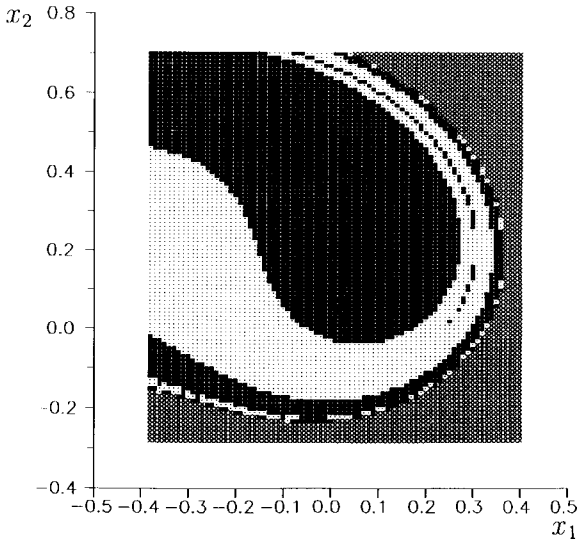

FIG. 10. Basins of coexisting attractors of Fig. 9. Here crosses denote the basin of the lower time-periodic state, black squares denote the basin of the upper time-periodic state, and dots denote the basin of the strange attractor.

sections between stable and unstable manifolds (separatrices). The predictions are in rather good agreement with numerical simulations. An important result is the coexistence of time-periodic states and a strange attractor. This coexistence may be explained by the identification of simple zeros of the Melnikov function for subharmonic orbits that lead to the appearance of time-periodic states in the chaotic region. This feature is more pronounced for low frequencies of modulations than for high frequencies. The coexisting basins of attraction (Fig. 10) show a high degree of intertwining between the two time-periodic states and the strange attractor, which indicates their fractal character. Also note that the prediction by Melnikov's method of the threshold of chaos may be useful in optical systems involving the control [17] or the suppression [27] of chaos when it is undesirable. In [27] Chizhevsky and Carbalán have experimentally observed that parametric resonances permit the suppression of chaos in a loss-modulated CO_2 laser. This combined effect of two time-periodic modulations to suppress chaos can be analyzed by using Melnikov's method. For instance, see Ref. [28] for an application of Melnikov's techniques to suppress chaos in the nonlinear Duffing equation under external modulations with two frequencies. It would now be interesting to analyze how the transverse instabilities [29] in the original problem may be affected by this temporal chaos since this study may be viewed as the behavior of localized structures, far from their centers, in spatially extended systems, with large aspect ratio [30]. The interaction between spatial instabilities and temporal chaos may lead to a shift of chaotic thresholds or even to the suppression of chaos. An analytical study of the spatial instabilities is in progress.

[1] H. M. Gibbs, S. L. McCall, and T. N. C. Venkatesan, Phys. Rev. Lett. **36**, 1135 (1976).

[2] R. Bonifacio and P. Meystre, Opt. Commun. **29**, 131 (1979).

[3] E. Abraham and S. D. Smith, Rep. Prog. Phys. **45**, 815 (1982).

[4] V. Molonney, H. M. Gibbs, and F. A. Hopf, in *Proceeding of the Topical Meeting on Optical Bistability, Rochester, 1983*, edited by C. M. Bowden, H. M. Gibbs, and S. L. McCall (Plenum, New York, 1984).

[5] K. Ikeda and O. Akomoto, Phys. Rev. Lett. **45**, 709 (1982).

[6] T. Erneux and P. Mandel, Phys. Rev. A **33**, 1777 (1986).

[7] J. Danckaert, G. Vitrant, R. Reinisch, and M. Giorgiou, Phys. Rev. A **48**, 2324 (1993).

[8] H. M. Gibbs, *Optical Bistability: Controlling Light with Light* (Academic, New York, 1985).

[9] W. Harshawardhan and G. S. Agrawal, Phys. Rev. A **53**, 1812 (1996).

[10] G. Assanto, in Proceeding of the International School of Physics ''Enrico Fermi,'' *Nonlinear Optical Materials: Principle and Applications*, Course CXXVI, Varenna, 1993 (IOS, Amsterdam, 1995).

[11] L. A. Lugiato and L. M. Narducci, Phys. Rev. A **32**, 1576 (1985); *Synergetics and Dynamic Instabilities*, edited by G. Caglioti, H. Haken, and L. A. Lugiato (North-Holland, Amsterdam, 1988); L. A. Orozco, H. J. Kimble, A. T. Rosenberger, L. A. Lugiato, M. L. Asquini, M. Brambilla, and L. M. Narducci, Phys. Rev. A **39**, 1235 (1989).

[12] B. Ségard and B. Macke, Phys. Rev. Lett. **60**, 412 (1988); B. Ségard, B. Macke, L. A. Lugiato, F. Prati, and M. Brambilla, Phys. Rev. A **39**, 703 (1989); B. Ségad, W. Sergent, B. Macke, and N. B. Abraham, *ibid.* **39**, 6029 (1989).

[13] S. Wiggins, *Chaotic Transport in Dynamical Systems* (Springer-Verlag, New York, 1992). See mainly pp. 64–79 for the application of Melnikov's method in transport theory.

[14] L. A. Lugiato, in *Progress in Optics*, edited by E. Wolf (North-Holland, Amsterdam, 1984), Vol. 21.

[15] R. Bonifacio, M. Gronchi, and L. A. Lugiato, Nuovo Cimento B **53**, 311 (1979).

[16] H. Gang, C. Z. Ning, and H. Haken, Phys. Rev. A **41**, 3975 (1990).

[17] M. Lefranc and P. Glorieux, Int. J. Bifurcation Chaos **3**, 643 (1993); M. Lefranc, P. Glorieux, F. Papoff, F. Molesti, and E. Arimendo, Phys. Rev. Lett. **73**, 1364 (1994).

[18] J. Zemmouri, W. Sergent, and B. Ségard, Opt. Commun. **84**, 199 (1991).

[19] L. A. Lugiato, M. Milani, and P. Meystre, Opt. Commun. **40**, 307 (1982).

[20] V. K. Melnikov, Trans. Moscow Math. Soc. **12**, 1 (1963).

[21] J. Guckenheimer and P. J. Holmes, *Nonlinear Oscillations, Dynamical Systems and Bifurcation of Vector Fields* (Springer-Verlag, New York, 1983).

[22] A. J. Lichtenberg and M. A. Lieberman, *Regular and Chaotic Dynamics*, 2nd ed. (Springer-Verlag, New York, 1992); S. Wiggins, *Introduction to Applied Nonlinear Dynamical Systems and Chaos* (Springer-Verlag, New York, 1990).

[23] M. Taki, J. C. Fernandez, and G. Reinisch, Phys. Rev. A **38**, 3086 (1988); M. N. Ouarzazi, P. A. Bois, and M. Taki, Eur. J. Mech. B, Fluids **13**, 423 (1994).

[24] V. G. Gelfreich, Physica D **101**, 227 (1996); C. Soto-Treviño

and T. J. Kaper, J. Math. Phys. (N.Y.) **37**, 6220 (1996).
[25] J. M. Malasoma, C. H. Lamarque, and L. Jezequel, Phys. Lett. A **186**, 126 (1994).
[26] J. Zemmouri, B. Ségard, B. Macke, and P. Glorieux, Opt. Commun. **79**, 431 (1990).
[27] V. N. Chizhevsky and R. Corbalán, Phys. Rev. A **53**, 1830 (1996).
[28] Y. Kivshar, F. Rödelsperger, and H. Benner, Phys. Rev. E **49**, 319 (1994).
[29] P. Mandel, M. Georgiou, and T. Erneux, Phys. Rev. A **47**, 4277 (1993).
[30] M. N. Ouarzazi, P. B. Bois, and M. Taki, Phys. Rev. A **53**, 4408 (1996).